Photodegradation of Crude Oil on a Solid Support

Maurizio D'Auria*, Lucia Emanuele, Rocco Racioppi, and **Vincenzina Velluzzi**
Dipartimento di Chimica, Università della Basilicata, Via N. Sauro 85, 85100 Potenza, Italy

Abstract

The modifications of crude oil after absorption on silica, montmorillonite, and zeolite were studied. Solid-phase microextraction gas chromatography–mass spectrometry analysis showed that some compounds are kept better by the solid support than other ones. The modifications that occurred were studied considering the relative amount of different classes of compounds, the number of compounds in function of the number of carbon atoms, and the relative amount in function of the number of carbon atoms for different classes of compounds (linear alkanes, branched alkanes, cyclic alkanes, aromatic hydrocarbons, and alkenes). The modifications which occurred after irradiation with a 125 W high pressure mercury arc towards Pyrex were studied. A global index of the modifications which occurred was proposed. All of the solids prevent photodegradation. Zeolite was the worst, while the most preservative effect was showed by montmorillonite.

Introduction

Photochemical and biological degradation are two methods of modifing crude oil in the environment. Accidental spilling of crude oil can induce extensive pollution events. The toxicity of crude oil could be modified after degradation and could increase. For these reasons, it is important to know the fate of all the components of crude oil when it is introduced into the environment.

Crude oil is subjected to some degradation processes. Biodegradation can be one of the most important processes in the environment. Photochemical degradation mediated by sunlight is an important pathway for the transformation of crude oil in tropical seawater, especially when the oil is rich in aromatics. Because chromophores are abundant in crude oils, many of the transformations are the result of direct photochemical processes.

In recent works, gas chromatography–mass spectrometry (GC–MS) analysis of crude oil after irradiation showed that the alkanes are unaffected, but the majority of the aromatic hydrocarbons have been converted to resins or polar molecules (1–4). These results are not in agreement with the observed photo-oxidation of *n*-pentadecane (5) and with the observed mineralization of *n*-alkanes in photocatalytic conditions (6,7).

A GC–MS analysis of water soluble fraction of crude oil showed that only the peaks with retention time between 8.46 and 12.36 min disappeared after 24 h under photolysis (8). These compounds are phenols and other aromatic compounds (tetramethylbenzene, naphthalene, isopropyl-dimetylbenzene). Preferential photo-oxidation of alkyl-substituted polycyclic aromatic hydrocarbons and heterocyclic aromatic was observed in comparison to their unsubstituted parent compounds (5,9).

Recently, we found that GC analysis in solution and headspace solid-phase microextraction (SPME)-GC analysis of a sample of crude oil gave different results (10). The SPME technique allowed the identification of a larger number of components

Table I. Adsorption and Photodegradation of Crude Oil on Silica*

No. carbon atoms	No. of comp. (neat)	No. of comp. (ads)†	No. of comp. (photo)†	Area % (neat)	Area % (ads)†	Area % (photo)†
C_3	1	0	0	0.09	0	0
C_4	1	0	0	1.00	0	0
C_5	2	2	2	2.54	5.24	2.14
C_6	4	4	4	5.42	15.08	8.13
C_7	6	4	5	8.26	22.36	12.64
C_8	8	8	12	14.10	16.62	18.96
C_9	7	7	11	16.56	11.91	12.70
C_{10}	10	9	13	17.33	12.02	14.03
C_{11}	7	10	8	6.59	7.39	8.49
C_{12}	5	10	9	3.60	4.31	6.30
C_{13}	1	8	10	0.54	2.68	5.77
C_{14}	2	7	7	0.36	1.42	4.05
C_{15}	1	3	5	0.05	0.64	2.32
C_{16}	0	1	6	0	0.06	1.04
C_{17}	0	1	2	0	0.01	0.20
C_{18}	0	0	1	0	0	0.37
C_{19}	0	0	1	0	0	0.03
C_{20}	0	2	2	0	0.27	0.76
C_{21}	0	0	1	0	0	0.26
C_{22}–C_{25}	0	0	0	0	0	0
C_{26}	0	0	1	0	0	0.08
C_{27}–C_{42}	0	0	0	0	0	0
C_{43}	0	0	1	0	0	0.11

*Distribution of the number of detected compounds and of the area per cent in function of the number of carbon atoms; †ads = adsorbed and photo = photodegraded.

* Author to whom correspondence should be addressed: email Maurizio.dauria@unibas.it.

than by using usual GC–MS. The method failed within the range C_{14}–C_{25}, where GC–MS in solution allowed us to obtain more representative results; on the contrary, SPME allowed us to obtain data on the presence of volatile compounds that could not be identified in GC–MS analysis in solution. Furthermore, in the range C_8–C_{12}, SPME allowed us to identify ~30 compounds that could not be identified in the GC–MS analysis in solution. Finally, SPME analysis identified some alkenes, while these compounds were not detected in GC–MS analysis in solution.

The fate of the crude oil under irradiation was studied by using both liquid injection and SPME methodologies (11). After the UV irradiation, the fraction present in the highest percentage shifted from C_8–C_9 fraction to C_{13} one, in GC–MS analysis in solution. An increase of the relative amount of the C_{13}–C_{25} fraction was observed, while a decrease in the relative amount of the C_7–C_{12} fractions was present. In HS–SPME analysis, the C_8–C_{10} fractions represented 53% of all the compounds detected. A decrease in the relative amount of the C_8–C_{10} fractions was observed, while C_{11}–C_{15} fractions increased. The irradiation with solar simulator of crude oil gave a mixture whose analysis using GC–MS in solution furnished the same type of results: the relative amounts of linear alkanes and aromatic compounds increased, while a sharp decrease of the relative amounts of branched and cyclic alkanes was observed. In the SPME analysis, a decreased relative amount of branched alkanes and alkenes and an increase of the relative amounts of cyclic alkanes and aromatic compounds were observed. These results could be explained, considering the high reactivity of branched and substituted cyclic alkanes towards radical reactions.

SPME-GC–MS can be used in the analysis of crude oil in contaminated soil (10). When adsorbed on soil, crude oil can be conserved for several years (12).

In this study, we report how SPME can be used in the analysis of both the adsorption of crude oil on solid supports and the photodegradation products on these supports. The results of this study could be useful to understand the mechanism of both

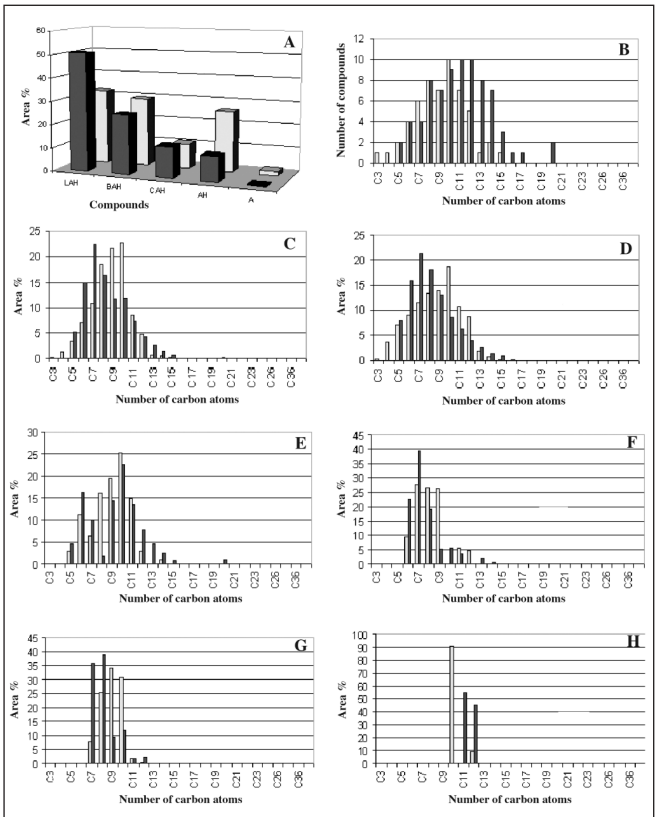

Figure 1. SPME-GC–MS analysis of crude oil before (lighter color) and after absorption on silica (darker color): composition of crude oil (lighter color) and absorbed crude oil (darker color), as a function of the type of compounds (A). LAH: linear aliphatic hydrocarbons; BAH: branched aliphatic hydrocarbons; CAH: cyclic aliphatic hydrocarbons; AH: aromatic hydrocarbons; A: alkenes; number of detected compounds in crude oil as a function of the number of carbon atoms (B); composition of crude oil as a function of the number of carbon atoms (C); composition of the linear aliphatic hydrocarbons fraction as a function of the number of carbon atoms (D); composition of the branched aliphatic hydrocarbons fraction as a function of the number of carbon atoms (E); composition of the cyclic hydrocarbons fraction as a function of the number of carbon atoms (F); composition of the aromatic hydrocarbons fraction as a function of the number of carbon atoms (G); composition of the alkenes fraction as a function of the number of carbon atoms (H).

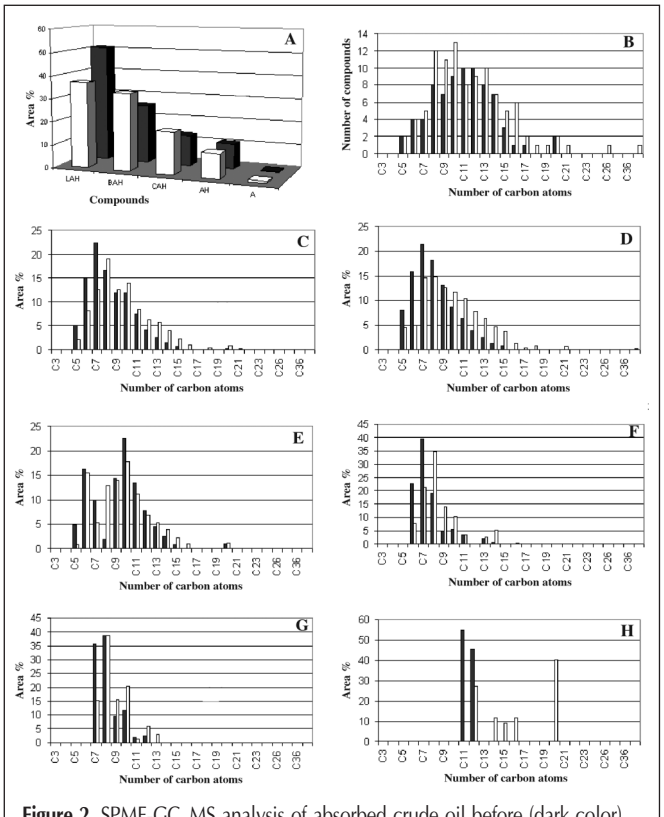

Figure 2. SPME-GC–MS analysis of absorbed crude oil before (dark color) and after irradiation on silica (light color) (A): composition of absorbed crude oil (dark color) and absorbed irradiated crude oil (light color), as a function of the type of compounds (B). LAH: linear aliphatic hydrocarbons; BAH: branched aliphatic hydrocarbons; CAH: cyclic aliphatic hydrocarbons; AH: aromatic hydrocarbons; A: alkenes; number of detected compounds in crude oil as a function of the number of carbon atoms (B); composition of crude oil as a function of the number of carbon atoms (C); composition of the linear aliphatic hydrocarbons fraction as a function of the number of carbon atoms (D); composition of the branched aliphatic hydrocarbons fraction as a function of the number of carbon atoms (E); composition of the cyclic hydrocarbons fraction as a function of the number of carbon atoms (F); composition of the aromatic hydrocarbons fraction as a function of the number of carbon atoms (G); composition of the alkenes fraction as a function of the number of carbon atoms (H).

adsorption of crude oil on a solid support and photodegradation on these supports.

Materials and Methods

In this study we used a sample of crude oil deriving from Centro Oli in Val D'Agri (Basilicata, Southern Italy). The sample showed in the elemental analysis the following composition: C, 85.13%; H, 12.31%; N, 0.00%; S, 2.74%.

Absorption of crude oil on solid support

The solid supports [silica (63–200 µm, purity > 99%, Aldrich), montmorillonite (surface area 250 m^2g^{-1}, mean particle size 3–4 µm, purity > 99%, Carlo Erba), and zeolite (NaY, mean particle size 7–10 µm, purity > 98%, Aldrich)] (2 g) and crude oil (0.2 g) were homogenized until a homogeneous color was observed. Both solid supports and crude oil were used without any pre-treatment.

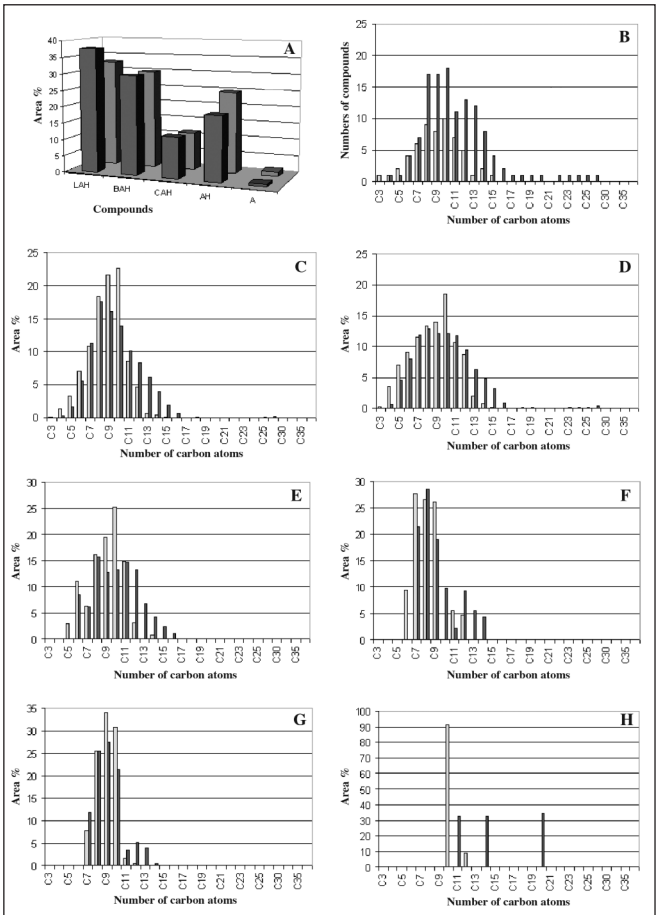

Figure 3. SPME-GC–MS analysis of crude oil before (lighter color) and after absorption on montmorillonte (dark color): composition of crude oil (light color) and absorbed crude oil (dark color), as a function of the type of compounds (A). LAH: linear aliphatic hydrocarbons; BAH: branched aliphatic hydrocarbons; CAH: cyclic aliphatic hydrocarbons; AH: aromatic hydrocarbons; A: alkenes; number of detected compounds in crude oil as a function of the number of carbon atoms (B); composition of crude oil as a function of the number of carbon atoms (C); composition of the linear aliphatic hydrocarbons fraction as a function of the number of carbon atoms (D); composition of the branched aliphatic hydrocarbons fraction as a function of the number of carbon atoms (E); composition of the cyclic hydrocarbons fraction as a function of the number of carbon atoms (F); composition of the aromatic hydrocarbons fraction as a function of the number of carbon atoms (G); composition of the alkenes fraction as a function of the number of carbon atoms (H).

Photodegradation of crude oil on solid support

The samples were irradiated in vials used for SPME analysis with a 125 W high pressure mercury arc (Helios-Italquartz, Milan, Italy) for five days. The vials were maintained in horizontal position, creating a homogeneous film. An SPME fiber coated with 100 µm of nongrafted poly(dimethylsiloxane) (PDMS) phase (Supelco 57300-U, mounted on a Supelco 57330 support) was conditioned for 1 h at 250°C in a stream of helium. A single fiber was used for the complete study. A blank run was performed after the analysis in order to confirm that no residual compound was polluting the fiber or the column. The headspace was generated from samples placed in a 20-mL flask. The flask was sealed and heated for 20 min in an aluminium block maintained at 45°C (40°C in the flask). During this time, the fiber was maintained over the sample. The fiber was then introduced into the injection port of a HP6890 plus GC equipped with a Phenomenex Zebron ZB-5 MS capillary column (30 m × 0.25 mm i.d. × 0.25 µm film thickness). As detector we used a HP5973 mass selective detector (mass range: 15-800 amu; scan rate: 1.9 scans/s; EM voltage: 1435); helium at 0.8 mL/min was used as carrier gas. The injection port, equipped with glass insert (internal diameter 0.75 mm), was splitless at 250°C. The desorption time of 1.0 min was used. Detector was maintained at 230°C. Oven was maintained at 40°C for 2 min, then the temperature increased until 250°C (8°C/min); finally, this temperature was maintained for 10 min. All the analyses were performed in triplicate (RSD 0.03%). The chromatograms obtained from the total ion current (TIC) were integrated without any correction for coelutions, and the results were expressed in arbitrary surface unites (asu). All the peaks were identified from their mass spectra by comparison with spectra in Wiley6N and NIST98 libraries.

Results and Discussion

The adsorption of crude oil on silica (SiO_2) gave the results reported in Figure 1 and Tables I and II. The absorption was not similar for all the classes of compounds. In Figure 1A, we observed that linear and cyclic alkanes were absorbed more selectively than branched alkanes and aromatic compounds. Alkenes were not absorbed. Considering the distribution of the compounds in function of the number of carbon atoms, we observed that (Figure 1B, Table I), while C_8 and C_{11} showed a decrease of the number of compounds, the C_{12}–C_{21} fractions showed a large increase of the number of compounds detected. The absorption on silica alloweds to bypass one of the problem detected with the use of SPME (11). In fact, we observed that SPME worked well with low boiling compounds, while it was not able to detect compounds with high molecular weight. The absorption on silica seems to avoid this problem.

However, the results reported in Figure 1C and Table I were

not in agreement with the previously reported assertions when we considered the quantitative evaluation of the adsorbed compounds. We noted that the C_6–C_8 fractions increased together with the C_{14}–C_{21} fractions, while the C_9–C_{13} fractions decreased. If we examined this distribution in the different class of compounds, we found that linear alkanes (Figure 1D, Table II) behaved as described before: the C_7–C_9 and C_{14}–C_{17} fractions increased and the C_{10}–C_{13} fractions decreased. Similar behaviors were observed for branched alkanes (Figure 1E, Table II) and cyclic alkanes (Figure 1F, Table II). In the case of aromatic compounds (Figure 1G, Table II), we observed an increase of the C_8, C_9, and C_{13} fractions and a sharp decrease of the C_{10}–C_{11} fractions.

After photodegradation with a 125 W mercury arc, we observed the situation depicted in Figure 2 (Tables I and II). Figure 2A reported the distribution of the photoproducts considering the different types of compounds. Linear alkanes decreased while we had an increase of branched and cyclic alkanes. The amount of aromatic alkanes did not undergo modifications, and we observed an increase in the amount of alkenes. These results were not in agreement with those obtained irradiating crude oil (11); in that case, we observed an increase of the amounts of linear alkanes and aromatic compounds and a decrease of the amounts of branched and cyclic alkanes. Furthermore, we observed a sharp reduction of the amount of alkenes; after irradiation, we did not find alkenes.

Then, the presence of crude oil absorbed on the solid support can modify the photochemical behavior and fate of the oil, changing the photochemical reactivity. In particular, it is surprising to note that we have no reduction of the amount of branched and cyclic alkanes (more reactive towards radical reactions) and the increase of the amount of alkenes, protected in silica towards photochemical reactions.

Considering the number of compounds as a function of the number of carbon atoms (Figure 2B, Table I), after irradiations, we observed an increase of the C_9–C_{11}, C_{13}, C_{15}–C_{20}, C_{22}–C_{38} fractions. On the other side, we observed a reduction of the C_{12} and C_{13} fractions. We had an increase of the number of compounds present in the mixture after irradiation. Considering the relative amount of the compounds as a function the number of carbon atoms (Figure 2C, Table I), the C_6–C_8 fractions decreased, while all the other fractions increased. Also in this case, we observed different behavior in comparison with that observed irradiating pure crude oil (11); in that case, we observed an increase of the C_4–C_6 fractions and a reduction of the C_7–C_{10} fractions. Furthermore, while the maximum was present in correspondence of the C_8 fraction, after irradiation it shifted at C_9 fraction. Irradiation of pure crude oil (11) gave a shift from C_{10} to C_8.

Considering the distribution as a function of the number of carbon atoms of linear alkanes (Figure 2D, Table II), the C_6–C_{10} fractions decreased while we observed an increase of the C_{11}–C_{38} fractions. In the case of branched alkanes (Figure 2E, Table II), we observed non-homogeneous behavior. C_6–C_8 and C_{10}–C_{13} fractions decreased. We had a sharp increase of the C_9 fraction and an increase of the C_{14}–C_{17} fractions. The observed increase of the amount of branched alkanes was mainly due to the increase

Table II. Adsorption and Photodegradation of Crude Oil on Silica*

	Linear alkanes			Branched alkanes			Cyclic alkanes			Aromatic			Alkenes		
No. CA†	Area % (neat)	Area % (ads)‡	Area % (photo)‡	Area % (neat)	Area % (ads)‡	Area % (photo)‡	Area % (neat)	Area % (ads)‡	Area % (photo)‡	Area % (neat)	Area % (ads)‡	Area % (photo)‡	Area % (neat)	Area % (ads)‡	Area % (photo)‡
C_3	0.32														
C_4	3.59														
C_5	7.06	7.95	4.53	2.98	4.76	0.86									
C_6	9.07	15.89	5.08	11.07	16.23	15.37	9.45	22.66	7.67						
C_7	11.58	21.38	14.68	6.37	9.99	5.29	27.73	39.52	21.37	7.74	35.79	15.16			
C_8	13.45	18.14	14.80	16.13	1.95	12.82	26.63	19.16	34.67	25.43	38.88	38.69			
C_9	13.98	12.98	12.57	19.42	14.39	13.88	26.14	5.09	13.95	34.02	9.51	15.39			
C_{10}	18.65	8.58	11.69	25.26	22.58	17.80		5.49	10.36	30.87	11.77	20.36	90.98		
C_{11}	10.69	6.30	10.36	14.88	13.42	11.13	5.52	3.59	3.59	1.55	1.78	1.36		54.55	
C_{12}	8.82	3.90	7.80	3.03	7.78	6.86	4.54			0.40	2.26	6.00	9.02	45.46	27.27
C_{13}	1.94	2.48	6.34		4.56	5.25		2.10	2.69			3.05			
C_{14}	0.68	1.34	4.62	0.89	2.56	3.84		0.70	5.38						11.69
C_{15}	0.18	0.91	3.78		0.72	2.16									9.09
C_{16}		0.13	1.30			1.10			0.33						11.69
C_{17}		0.03	0.39			0.19									
C_{18}			0.91												
C_{19}			0.06												
C_{20}					1.08	1.18									40.26
C_{21}			0.63												
C_{22}–C_{25}															
C_{26}			0.18												
C_{27}–C_{42}															
C_{43}			0.27												

* Distribution of the area per cent in function of the number of carbon atoms for type of compounds; † CA = carbon atoms; ‡ ads = adsorbed and photo = photodegraded.

of the C_9 fraction. The photochemical behavior of cyclic alkanes is depicted in Figure 2F and Table II. In this case, we had a reduction of C_7 and C_8 fractions and a sharp increase of C_9 fraction.

Figure 2G and Table II collect the results obtained with the aromatic fraction. We observed a sharp decrease in the amount of the C_8 fraction and an increase of the C_{10}, C_{11}, C_{13}, and C_{15} ones.

As reported earlier, we found that alkenes were recovered after irradiation. Also, this class of compound underwent some modifications during irradiation (Figure 2H, Table II). While in absorbed crude oil we observed C_{12} and C_{13} alkenes, after irradiation, the C_{12} fraction did not exist and alkenes with 15, 16, 17, and 21 carbon atoms appeared.

The adsorption on silica seems to modify the photochemical behavior of crude oil. The modifications that occurred in the composition of crude oil are quite different in this case (in comparison with those that occurred after irradiation of pure crude oil). In particular, we observed a decrease of the amount of compounds with low molecular weight and an increase of the fraction containing high molecular weight compounds. The photochemical behavior seems to be related to radical coupling reactions and not to photodegradation reactions or photoxidation reactions. It is noteworthy that the alkene fraction does not disappear after irradiation; on the contrary, new compounds with higher molecular weights appears in the reaction mixture.

To confirm this behavior we tested the photochemistry of crude oil on other absorbed phases that were able to simulate the absorption on soil. For this purpose, we used montmorillonite, an hydrate sodium calcium aluminium magnesium silicate hydride [$NaClAl_6Mg_6(Si_4O_{10})_3(OH)_6 \cdot nH_2O$]. Montmorillonite is

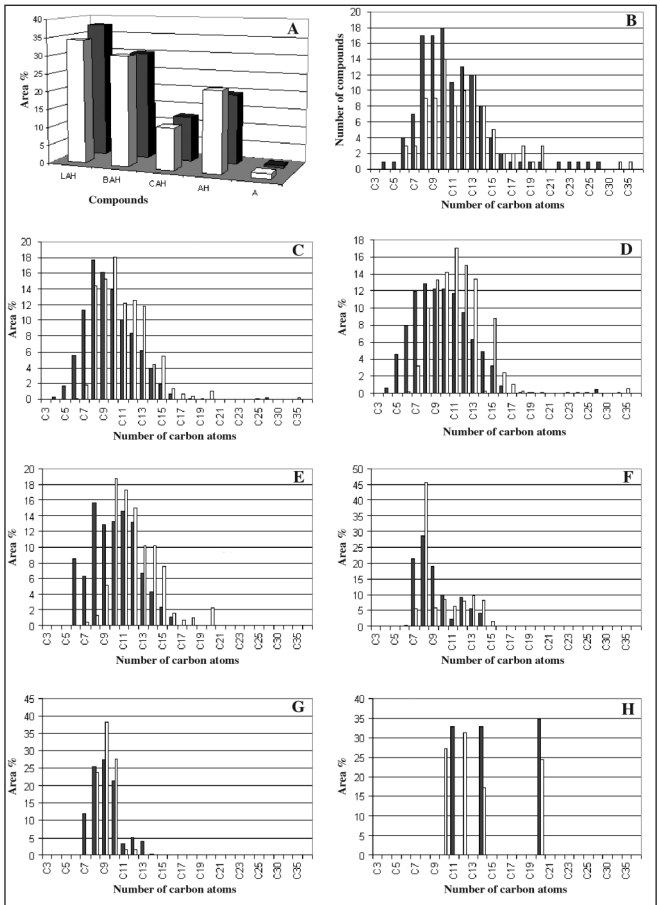

Figure 4. SPME-GC–MS analysis of absorbed crude oil before (dark color) and after irradiation on montmorillonite (light color): composition of absorbed crude oil (dark color) and absorbed irradiated crude oil (light color), as a function of the type of compounds (A). LAH: linear aliphatic hydrocarbons; BAH: branched aliphatic hydrocarbons; CAH: cyclic aliphatic hydrocarbons; AH: aromatic hydrocarbons; A: alkenes; number of detected compounds in crude oil as a function of the number of carbon atoms (B); composition of crude oil as a function of the number of carbon atoms (C); composition of the linear aliphatic hydrocarbons fraction as a function of the number of carbon atoms (D); composition of the branched aliphatic hydrocarbons fraction as a function of the number of carbon atoms (E); composition of the cyclic hydrocarbons fraction as a function of the number of carbon atoms (F); composition of the aromatic hydrocarbons fraction as a function of the number of carbon atoms (G); composition of the alkenes fraction as a function of the number of carbon atoms (H).

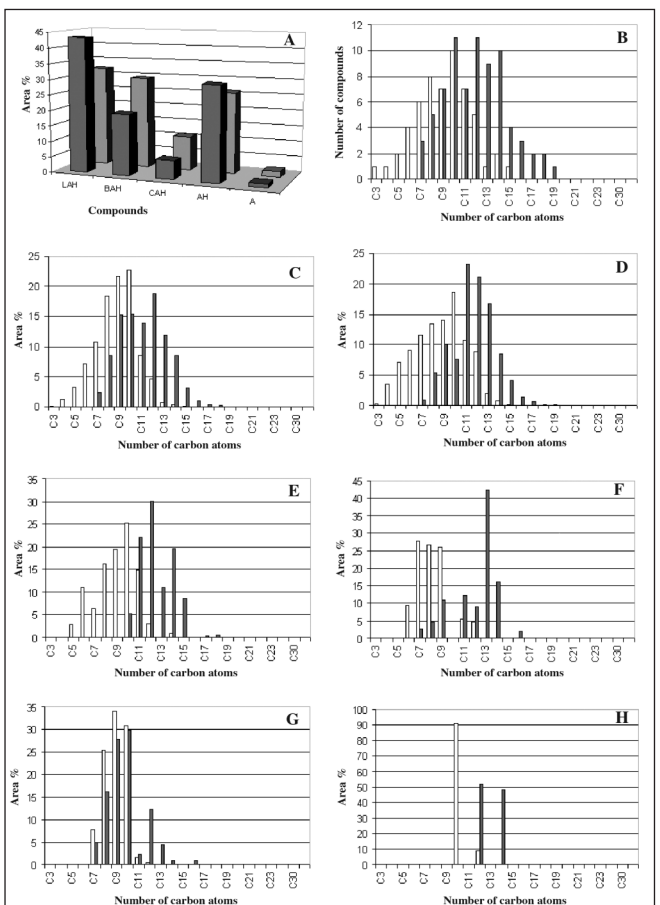

Figure 5. SPME-GC–MS analysis of crude oil before (lighter color) and after absorption on zeolite NaY (darker color): composition of crude oil (lighter color) and absorbed crude oil (darkeer color), as a function of the type of compounds (A). LAH: linear aliphatic hydrocarbons; BAH: branched aliphatic hydrocarbons; CAH: cyclic aliphatic hydrocarbons; AH: aromatic hydrocarbons; A: alkenes; number of detected compounds in crude oil as a function of the number of carbon atoms (B); composition of crude oil as a function of the number of carbon atoms (C); composition of the linear aliphatic hydrocarbons fraction as a function of the number of carbon atoms (D); composition of the branched aliphatic hydrocarbons fraction as a function of the number of carbon atoms (E); composition of the cyclic hydrocarbons fraction as a function of the number of carbon atoms (F); composition of the aromatic hydrocarbons fraction as a function of the number of carbon atoms (G); composition of the alkenes fraction as a function of the number of carbon atoms (H).

a member of the general mineral group called clays. It typically forms microscopic or at least very small platy micaceous crystals. The water content is variable, and, in fact, when water is adsorbed by the crystals, they tend to swell to several times their original volume.

The absorption of crude oil on montmorillonite gave the results reported in Figure 3 (Tables III and IV). As in the case of silica, the adsorption was not similar for the entire class of compounds. In Figure 3A, we observed that linear compounds was adsorbed more selectively than aromatic ones. Branched and cyclic alkanes were adsorbed maintaining the same amounts of the pure crude oil. Considering the distribution of the compounds as a function of the number of carbon atoms, we observed (Figure 3B, Table III) that the C_7–C_{29} fractions showed a large increase in the number of compounds detected.

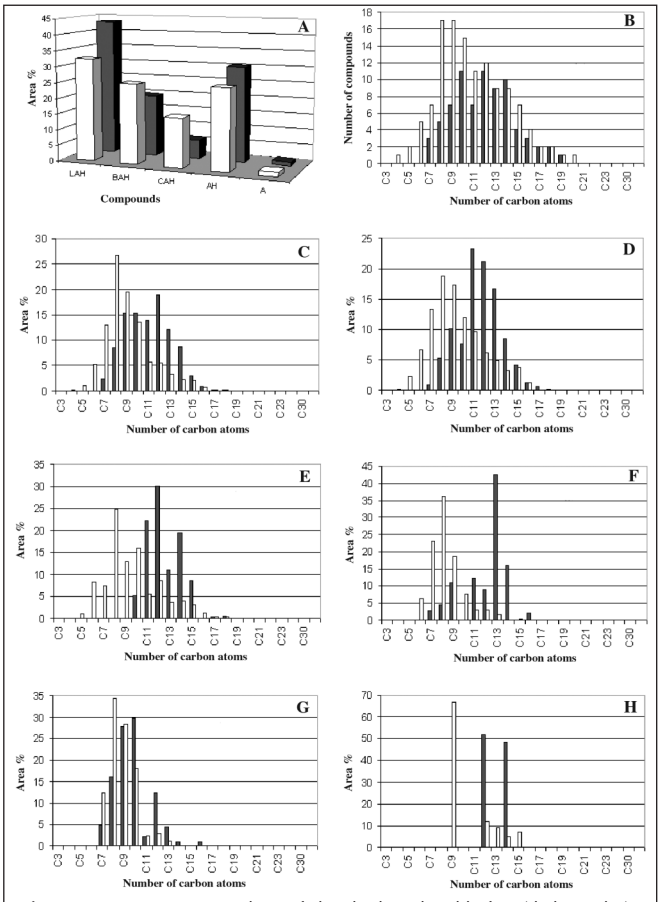

Figure 6. SPME-GC–MS analysis of absorbed crude oil before (darker color) and after irradiation on zeolite NaY (lighter color): composition of absorbed crude oil (darker color) and absorbed irradiated crude oil (lighter color), as a function of the type of compounds (A). LAH: linear aliphatic hydrocarbons; BAH: branched aliphatic hydrocarbons; CAH: cyclic aliphatic hydrocarbons; AH: aromatic hydrocarbons; A: alkenes; number of detected compounds in crude oil as a function of the number of carbon atoms (B); composition of crude oil as a function of the number of carbon atoms (C); composition of the linear aliphatic hydrocarbons fraction as a function of the number of carbon atoms (D); composition of the branched aliphatic hydrocarbons fraction as a function of the number of carbon atoms (E); composition of the cyclic hydrocarbons fraction as a function of the number of carbon atoms (F); composition of the aromatic hydrocarbons fraction as a function of the number of carbon atoms (G); composition of the alkenes fraction as a function of the number of carbon atoms (H).

Figure 3C (Table III) shows the distribution of the relative amounts of compounds as a function of the number of carbon atoms. We noted that the C_7 fraction increased together with the C_{11}–C_{16} fractions, while the C_8–C_{10} fractions decreased. If we examined this distribution in the different class of compounds, we found that linear alkanes (Figure 3D, Table IV) behaved as described before: the C_7 and C_{11}–C_{16} fractions increased and the C_8–C_{10} fractions decreased. In the case of branched alkanes (Figure 3E, Table IV), we observed an increase of the C_{12}–C_{17} fractions and a decrease in the C_8–C_{10} fractions. Considering cyclic alkanes (Figure 3F, Table IV), we have a complex behavior: the C_6 fraction disappeared and the C_7, C_9, and C_{11} fractions decreased; on the other side, the C_8 and C_{10} fractions together with the C_{12}–C_{14} fractions increased. In particular, the C_{10} fraction was completely absent in the original sample. In the case of aromatic compounds (Figure 3G, Table IV), we observed an increase of the C_7 and C_{11}–C_{15} fractions and a decrease of the C_9–C_{10} fractions.

Figure 4 and Tables III and IV report the results obtained by analysing the absorbed crude oil after irradiation. Also in this case, we observed some modifications in the composition of crude oil. Figure 4A reports the composition of crude oil considering some different classes of compounds. We observed, as in

Table III. Adsorption and Photodegradation of Crude Oil on Montmorillonite*

No. CA†	NC‡ (neat)	NC‡ (ads)§	NC‡ (photo)§	Area % (neat)	Area % (ads)§	Area % (photo)‡
C_3	1	0	0	0.09	0	0
C_4	1	1	0	1.00	0.24	0
C_5	2	1	0	2.54	1.71	0
C_6	4	4	3	5.42	5.55	0.11
C_7	6	7	3	8.26	11.33	1.89
C_8	8	17	9	14.10	17.67	14.41
C_9	7	17	9	16.56	16.12	15.34
C_{10}	10	18	14	17.33	13.93	18.09
C_{11}	7	11	8	6.59	10.15	12.22
C_{12}	5	13	10	3.60	8.37	12.58
C_{13}	1	12	12	0.54	6.16	11.83
C_{14}	2	8	8	0.36	3.93	4.39
C_{15}	1	4	5	0.05	1.92	5.52
C_{16}	0	2	2	0	0.68	1.31
C_{17}	0	1	2	0	0.04	0.62
C_{18}	0	1	3	0	0.05	0.42
C_{19}	0	1	1	0	0.02	0.06
C_{20}	0	1	3	0	0.01	1.05
C_{21}	0	0	0	0	0	0
C_{22}	0	1	0	0	0.01	0
C_{23}	0	1	0	0	0.02	0
C_{24}	0	1	0	0	0.04	0
C_{25}	0	1	0	0	0.05	0
C_{26}	0	1	0	0	0.17	0
C_{27}–C_{33}	0	0	0	0	0	0
C_{34}	0	0	1	0	0	0.01
C_{35}	0	0	1	0	0	0.17

* Distribution of the number of detected compounds and of the area per cent in function of the number of carbon atoms; † CA = carbon atoms; ‡ NC = number of compounds; § ads = adsorbed; photo = photodegraded.

the case of silica (Figure 2A), a decrease of the amount of linear aliphatic alkanes. On the contrary, we did not observe modifications in the amount of branched alkanes. Furthermore, while in the case of silica, we observed an increase of the amount of cyclic alkanes;the absorption on montmorillonite induced a reduction of the amount of this class of compounds. Finally, we observed an increase in the amount of aromatic hydrocarbons.

Considering the number of compounds as a function of the number of carbon atoms (Figure 4B, Table III), we observed a decrease of the number of compounds in the C_4–C_{12} fractions. We observed an increase in the number of components only in the C_{15}, C_{17}, C_{18}, and C_{20} fractions. We observed also one component in C_{34} and C_{35} fractions.

In Figure 4C and Table III, we report the relative amount as a function of the number of carbon atoms. We observed a decrease of the amounts of the C_4–C_9 fractions and an increase in the C_{10}–C_{20} fractions. We observed a shift of the distribution towards higher number of carbon atoms. Before the irradiation, the maximum of distribution was at C_8 and it shifted at C_{10} after the irradiation.

Considering only linear alkanes (Figure 4D, Table IV), also in this case we observed a shift of the distribution towards higher number of carbon atoms. We observed a decrease in the C_4–C_8 fractions and in increase in the C_9–C_{18} fractions. The maximum of the distribution was at C_7 before the irradiation and it shifted at C_{12} after the irradiation. A similar situation was observed in the composition of branched alkanes [we have to note that the total amount (Figure 4A) did not change] (Figure 4E, Table IV). Also in this case, we observed a decrease of the amount in C_5–C_9 fractions and an increase in the C_{10}–C_{20} fractions. Also in this case, we have a shift of the maximum of the distribution from C_8 (before the irradiation) to C_{10} (after the irradiation).

In the case of cyclic alkanes we observed a very complex behavior (Figure 4F, Table IV). We observed an increase in the C_8, C_{11}, C_{13}–C_{15} fractions, but a decrease in the C_7, C_9, C_{10}, and C_{12} fractions. A similar situation was observed in the class of aromatic compounds (Figure 4G, Table IV). In this case, the C_7 and C_{13} fractions disappeared after the irradiation, and we observed a reduction in the amount of the C_8, C_{11}, and C_{12} fractions. We observed an increase only in the C_9 and C_{10} fractions. Finally, in Figure 4H and Table IV we reported the behavior of the alkenes found in crude oil. The C_{11} fraction disappeared, while C_{14} and C_{20} decreased. On the contrary, we observed the formation of alkenes with 10 and 12 carbon atoms.

Finally, we used zeolite [NaY, $Na_{56}(Al_2O_3)_{56}(SiO_2)_{136}{\cdot}253H_2O$] as absorbing phase. Zeolites are microporous crystalline aluminosilicates with structural features that make them attractive hosts for photochemical applications. The topological structure of Y-type zeolite consists of an interconnected three-dimensional network of relatively large spherical cavities, termed primary

Table IV. Adsorption and Photodegradation of Crude Oil on Montmorillonite*

	Linear alkanes			Branched alkanes			Cyclic alkanes			Aromatic			Alkenes		
No. CA	Area % (neat)	Area % (ads)†	Area % (photo)†	Area % (neat)	Area % (ads)†	Area % (photo)†	Area % (neat)	Area % (ads)†	Area % (photo)†	Area % (neat)	Area % (ads)†	Area % (photo)†	Area % (neat)	Area % (ads)†	Area % (photo)†
C_3	0.32														
C_4	3.59	0.64													
C_5	7.06	4.53		2.98											
C_6	9.07	7.96	0.24	11.07	8.52	0.05	9.45		0.12						
C_7	11.58	11.98	3.21	6.37	6.26	0.41	27.73	21.42	5.69	7.74	11.89				
C_8	13.45	12.88	10.00	16.13	15.70	1.33	26.63	28.59	45.76	25.43	25.39	23.75			
C_9	13.98	12.24	13.30	19.42	12.84	5.14	26.14	18.96	5.81	34.02	27.44	38.28			
C_{10}	18.65	12.24	14.19	25.26	13.24	18.72		9.82	8.48	30.87	21.34	27.63	90.98		27.27
C_{11}	10.69	11.75	17.04	14.88	14.61	17.34	5.52	2.16	6.30	1.55	3.36	1.63		32.69	
C_{12}	8.82	9.51	15.01	3.03	13.16	14.95	4.54	9.14	7.99	0.40	5.10	1.69	9.02		31.31
C_{13}	1.94	6.33	13.34		6.66	10.14		5.60	9.81		3.98	7.02			
C_{14}	0.68	4.85	0.29	0.89	4.32	10.14		4.32	8.35		0.37			32.69	17.17
C_{15}	0.18	3.21	8.78		2.38	7.57			1.70						
C_{16}		0.90	2.40		1.13	1.61									
C_{17}			1.14		0.12	0.73									
C_{18}		0.13	0.33			1.01									
C_{19}		006	0.16												
C_{20}		0.03	0.04			2.29								34.62	24.24
C_{21}															
C_{22}		0.03													
C_{23}		0.06													
C_{24}		0.10													
C_{25}		0.13													
C_{26}		0.45													
C_{27}–C_{33}															
C_{34}			0.04												
C_{35}			0.49												

* Distribution of the area per cent in function of the number of carbon atoms for type of compounds;† ads = adsorbed; photo = photodegraded.

super-cages (diameter of ~ $13 \cdot 10^{-10}$ m); each supercage is connected tetrahedrally to four other secondary super-cages through $7.4–7.6 \times 10^{-10}$ m windows. Extra framework cations are necessary for the neutralization of charges due to the presence of tetrahedral aluminium. These cations can easily interact with guest molecules. To charge-compensating cations are known to occupy three different positions in the internal structure of Y-zeolites; the first type (site I), with 16 cations per unit cell, is located on the hexagonal prism faces between the sodalite units. The second type (site II), with 32 cations per unit cell, is located in the open hexagonal faces. The third type (site III), with eight cations per unit cell, is located in the walls of the largest cavity. Only cations at sites II and III are expected to be readily accessible to the organic molecule adsorbed within a super-cage.

Table V. Adsorption/Photodegradation of Crude Oil on Zeolite*

No. CA†	NC† (neat)	NC† (ads)‡	NC† (photo)‡	Area % (neat)	Area % (ads)‡	Area % (photo)‡
C_3	1	0	0	0.09	0	0
C_4	1	0	1	1.00	0	0.08
C_5	2	0	2	2.54	0	1.07
C_6	4	0	5	5.42	0	5.24
C_7	6	3	7	8.26	2.44	12.93
C_8	8	5	17	14.10	8.57	26.70
C_9	7	7	17	16.56	15.31	19.54
C_{10}	10	11	15	17.33	15.46	13.51
C_{11}	7	7	11	6.59	13.95	5.61
C_{12}	5	11	12	3.60	18.91	5.58
C_{13}	1	9	9	0.54	12.01	3.21
C_{14}	2	10	9	0.36	8.62	2.22
C_{15}	1	4	7	0.05	3.06	2.18
C_{16}	0	3	4	0	1.00	0.76
C_{17}	0	2	2	0	0.31	0.10
C_{18}	0	2	2	0	0.16	0.11
C_{19}	0	1	1	0	0.04	0.05
C_{20}	0	0	1	0	0	0.02

* Distribution of the number of detected compounds and of the area per cent in function of the number of carbon atoms; † CA = carbon atoms; NC = number of compounds; ads = adsorbed; photo = photodegraded.

Figure 5, Table V and VI collect the results obtained on absorption of crude oil on the zeolite. Figure 5A reports the distribution of the compounds considering the different classes of compounds. As in the cases of silica and montmorillonite, the absorption induced an increase of the relative amount of linear alkanes and a decrease of the amount of branched alkanes. In this case, we observed a reduction of the relative amount of cyclic alkanes and an increase of the relative amount of aromatic compounds, never observed before. Considering the number of compounds present as a function of the number of carbon atoms (Figure 5B, Table V), we had a sharp decrease in the $C_3–C_8$ range and an increase in the C_{10} and $C_{12}–C_{19}$ fractions. The same situation was obtained considering the relative amount of the compounds in function of the number of carbon atoms (Figure 5C, Table V). We had a sharp decrease in the $C_3–C_{10}$ range and an increase in the $C_{11}–C_{19}$ range. The same behavior was observed considering the relative amount of linear alkanes as a function of the number of carbon atoms (Figure 5D, Table VI). In the case of branched alkanes (Figure 5E, Table VI), we observed that the $C_5–C_9$ fractions disappeared, the C_{10} fraction decreased, and the $C_{11}–C_{19}$ fractions increased. In the case of cyclic alkanes (Figure 5F, Table VI), we observed a reduction of the $C_6–C_9$ fractions and an increase in the $C_{11}–C_{17}$ fractions. Finally, in the case of aromatic compounds (Figure 5G, Table VI), we observed a decrease

Table VI. Adsorption and Photodegradation of Crude Oil on Zeolite*

	Linear alkanes			Branched alkanes			Cyclic alkanes			Aromatic			Alkenes		
No. CA	Area % (neat)	Area % (ads)†	Area % (photo)†	Area % (neat)	Area % (ads)†	Area % (photo)†	Area % (neat)	Area % (ads)†	Area % (photo)†	Area % (neat)	Area % (ads)†	Area % (photo)†	Area % (neat)	Area % (ads)†	Area % (photo)†
C_3	0.32														
C_4	3.59		0.25												
C_5	7.06		2.32	2.98		1.22									
C_6	9.07		6.67	11.07		8.22	9.45		6.29						
C_7	11.58	0.97	13.42	6.37		7.38	27.73	2.75	23.11	7.74	4.92	12.38			
C_8	13.45	5.32	18.85	16.13		24.77	26.63	4.50	36.16	25.43	16.14	34.40			
C_9	13.98	10.11	17.30	19.42	0.15	12.85	26.14	11.00	18.71	34.02	27.82	28.42			66.67
C_{10}	18.65	7.60	12.00	25.26	5.15	16.12			7.70	30.87	29.78	17.98	90.98		
C_{11}	10.69	23.19	9.61	14.88	22.06	5.51	5.52	12.25	2.99	1.55	2.22	2.35			
C_{12}	8.82	21.12	6.16	3.03	30.04	8.65	4.54	9.00	2.91	0.40	12.34	3.01	9.02	51.81	12.12
C_{13}	1.94	16.70	4.97		11.10	3.60		42.50	1.73		4.41	1.13			9.09
C_{14}	0.68	8.47	3.34	0.89	19.52	4.07		16.00			0.98	0.09		48.19	5.05
C_{15}	0.18	4.22	3.77		8.64	3.13			0.39						7.07
C_{16}		1.37	1.34			1.26		2.00			0.98				
C_{17}		0.67			0.36	0.37									
C_{18}		0.17			0.58	0.42									
C_{19}		0.10				0.19									
C_{20}						0.09									

* Distribution of the area per cent in function of the number of carbon atoms for type of compounds.† ads = adsorbed; photo = photodegraded.

Table VII. Variation of the Composition of Crude Oil After Irradiation Considering Different Classes of Compounds

Experiment Variation |Δ|	Linear alkanes	Branched alkanes	Cyclic alkanes	Aromatic hydrocarbons	Alkenes	Σ|Δ|
Crude oil	10.39	10.48	2.36	5.81	3.46	32.5
Crude oil (Silica)	13.56	8.06	5.02	0.10	0.58	27.32
Crude oil (Montmorillonite)	3.32	0.49	0.77	2.85	0.75	8.18
Crude oil (Zeolite)	10.77	5.73	9.53	4.62	0.14	30.79

in the C_7–C_{10} fractions and an increase in the C_{11}–C_{17} fractions.

Figure 6 collects the results obtained irradiating crude oil adsorbed on zeolite (Tables V and VI). Figure 6A shows the distribution of crude oil considering different types of compounds before and after irradiation. We observed a sharp decrease in the amount of linear alkanes and an increase in the amounts of branched and cyclic alkanes. We observed also a reduction of the amount of aromatic compounds. It is noteworthy that the low amount of alkenes was not modified; however, its composition was modified (Figure 6H, Table VI).

Considering the distribution of the number of compounds in function of the number of carbon atoms (Figure 6B, Table V), we observed an increase of the C_5–C_{13} fractions and of the C_{16}, C_{17}, and C_{21} fractions. We had a reduction only in the C_{15} fraction. This behavior was not confirmed considering the relative amounts as a function of the number of carbon atoms (Figure 6C, Table V). In this case, we observed an increase of the C_5–C_{10} fractions and a decrease of the C_{11}–C_{19} fractions. This distribution is very similar to that obtained considering the amounts of linear alkanes (Figure 6D, Table VI). We observed an increase in the C_5–C_{11} fractions and a decrease in the C_{12}–C_{15} fractions.

In the case of branched alkanes (Figure 6E, Table VI), we observed a sharp increase of the C_6–C_{11} fractions. Also in the case of cyclic alkanes, we observed a sharp increase in low molecular weight fractions (C_7–C_{11}) and a sharp decrease in the C_{12}–C_{15} fractions (Figure 6F, Table VI). In the case of aromatic compounds, we observed an increase in the C_8–C_{10} fractions and a decrease in the other fractions (Figure 6G, Table VI).

Conclusion

We demonstrated that the photodegradation of crude oil on solid support depends on the nature of the solid support. We can propose that photodegradation of crude oil on a soil after an accidental oil spilling should depend on the nature of the soil. It is noteworthy that the photodegradation is very different if performed on crude oil and on crude oil adsorbed on a solid support.

We have to consider this possible question: does the adsorption of the crude oil on a support make easier the photodegradation or does the solid support protect the crude oil towards/from the photodegradation? Certainly, the absorption on a solid support protects alkenes towards photochemical reactions. This very low fraction in crude oil disappeared after irradiation of crude oil, and we did not find this behavior when crude oil was absorbed on a solid. To answer the question, we need of a global index able to describe the variation of the composition of crude oil. We think that this global index could Σ |Δ|, where, with |Δ|; we intend the modulus of the variation between the crude oil or absorbed crude oil and that after irradiation. The results are reported in Table VII. We consider the variation observed in the amount of the different classes of compounds after irradiation (Figures 2A, 4A, and 6A).

We can see that all the solid prevent photodegradation. Zeolite was the worst, while the most preservative role was shown by montmorillonite.

References

1. R.C. Prince, R.M. Garrett, R.E. Bare, M.J. Grossman, T. Townsend, J.M. Suflita, K. Lee, E.H. Owens, G.A. Sergy, J.F. Braddock, J.E. Lindstrom, and R.R. Lessard. The role of photooxidation and biodegradation in long-term weathering of crude and heavy fuel oils. *Spill Sci. Technol. Bull.* **8:** 145–56 (2003).
2. R. Lee. Photo-oxidation and photo-toxicity of crude and refined oils. *Spill Sci. Technol. Bull.* **8:** 157–62 (2003).
3. G. S. Douglas, E. H. Owens, J. Hardenstine, and R. G. Princes. The OSSA II pipeline oil spill: the character and wheatering of the spilled oil. *Spill Sci. Technol. Bull.* **7:** 135–48 (2002).
4. R.M. Garrett, I.J. Pickering, C.E. Haith, and R.C. Prince. Photooxidation of crude oils. *Environ. Sci. Technol.* **32:** 3719–23 (1998).
5. M. Ehrhardt and G. Patrick. On the sensitized photo-oxidation of alkylbenzenes in seawater. *Mar. Chem.* **15:** 47–58 (1984).
6. I.R. Bellobono, F. Morazzoni, R. Bianchi, E.S. Mangone, R. Stanescu, C. Costache, and P.M. Tozzi. Laboratoy-scale photomineralisation of *n*-alkanes in aqueous solutions, by photocatalytic membranes immolising titanium dioxide. *Int. J. Photoenergy* **7:** 79–85 (2005).
7. I.R. Bellobono, R. Stanescu, C. Costache, C. Canevali, F. Morazzoni, R. Scotti, R. Bianchi, E.S. Mangone, G. de Martini, and P.M. Tozzi. Laboratory-scale photomineralization of *n*-alkanes in gaseous phase by photocatalytic membranes immobilizing titanium dioxide. *Int. J. Photoenergy* ID 73167 (2006).
8. R.L. Ziolli and W.F. Jardim. Photochemical transformations of water-soluble fraction (WSF) of crude oil in marine waters. A comparison between photolysis and accelerated degradation with TiO2 using GC-MS and UVF. *J. Photochem. Photobiol. A: Chem.* **155:** 243–52 (2003).
9. M.G. Ehrhardt, K.A. Burns, and M.C. Bicego. Sunlight-induced compositional alterations in the seawater-soluble fraction of a crude oil. *Mar. Chem.* **37:** 53–64 (1992).
10. M. D'Auria, R. Racioppi, and E. Velluzzi. A comparison of results obtained using liquid injection and headspace solid phase microextraction for crude oil analysis by gas chromatography with mass spectrometer detector. *J. Chromatogr. Sci.* **46:** 332–338 (2008).
11. M. D'Auria, R. Racioppi, and V. Velluzzi. Photo-degradation of crude oil: liquid injection and headspace solid phase microextraction for crude oil analysis by gas chromatography with mass spectrometer detector. *J. Chromatogr. Sci.* **46:** 339–344 (2008).
12. A. Scopa, G. Salzano, L. Scrano, S. A. Bufo, and M. G. Bonomo. Preliminary assessment of microbial community recovery after an accidental oil spill by molecular analysis. *Fresenius Environ. Bull.* **15:** 675–81 (2006).

Manuscript received November 5, 2007;
revision received February 5, 2008.